Available online at www.sciencedirect.com
ScienceDirect
Journal of Power Sources 164 (2007) 328–335
JOURNAL OF POWER SOURCES
www.elsevier.com/locate/jpowsour

Toward autonomous control of microreactor system for steam reforming of methanol

W.C. Shin, R.S. Besser *

New Jersey Center for Microchemical Systems, Chemical, Biomedical and Materials Engineering, Stevens Institute of Technology, Castle Point on Hudson, Hoboken, NJ 07030, USA

Received 25 August 2006; accepted 1 October 2006
Available online 28 November 2006

Abstract

Since the introduction of microchemical systems (MCS) in the last decade, it has been recognized that one of the most crucial challenges is the implementation of an appropriate control strategy. A novel study in realizing a controllable miniature chemical plant for a small-scale hydrogen source for fuel cells is presented. Catalytic steam reforming (SR) reaction of a methanol–water mixture was the model reaction studied. A microscaled reactor, sensors and actuators, were successfully prepared and integrated by using microelectromechanical systems (MEMS) technology. Microfabricated system components were then interconnected with a comprehensive control algorithm which could form the basis for an eventual autonomous, self-contained system.

MCS represent a concept wherein precisely microfabricated fluid passages and reaction zones are integrated with sensors and actuators. Having an appropriate control strategy for the entire system of MCS is therefore a significant technical challenge. Although numerous MEMS-based examples of sensors and actuators exist for control of pressure, temperature and flow, there are few cases where these components have been combined with chemical reaction units and control algorithms into MCS. In this study, control of temperature and flow allows the hydrogen production rate to be modulated in a suitable fashion to support proton exchange fuel cell operation as a model. The reaction characteristics with temperature and flow changes, cold start-up behavior and the response to rapid changes in hydrogen demand were investigated. The control scheme implemented showed potential for autonomous control of fuel processing and other microchemical processing applications.

Keywords: MEMS; Microreactor; Microchemical systems; PID control; Steam reforming; Fuel cell

1. Introduction

Microchemical systems, possessing attractive benefits due to their microscale characteristic geometry, have generated much interest recently [1–4]. One of the key challenges to MCS is the establishment of appropriate control strategies which accommodate their unique characteristics such as faster system response, increased sensitivity to system perturbations and shorter start-up time [5,6]. The ultimate goal of this work is to develop an understanding of how these distinct control attributes differ from those of conventional chemical systems and to propose implementations in actual MCS. The methodology we have taken involves the fabrication of a complete MCS-based process, tuning of specific control loops within the process, rationalizing these characteristics in comparison to larger systems, building a comprehensive control algorithm for typical operating scenarios, and finally, projecting the future implementation of MCS-based processes for practical small power sources.

Feedback control plays an important role in ensuring the proper functionality of microdevices and is greatly enabled by both sensing and actuation capabilities. Among many sophisticated control strategies that have been developed in the last decades, PID controllers are the most adopted in practical use [7–9]. This seems to be because PID controllers possess functional simplicity, robustness and acceptable performance for a wide range of industrial applications, while their adaptation is well known among industrial practitioners. Economically, PID controllers provide a cost/benefit performance that is difficult to achieve with other kinds of controllers [10]. Furthermore, because of the variety of PID controllers in practice and the various natures of processes, extensive research efforts have

* Corresponding author. Tel.: +1 201 216 5257; fax: +1 201 216 8306.
E-mail address: rbesser@stevens.edu (R.S. Besser).

0378-7753/$ – see front matter © 2006 Elsevier B.V. All rights reserved.
doi:10.1016/j.jpowsour.2006.10.021

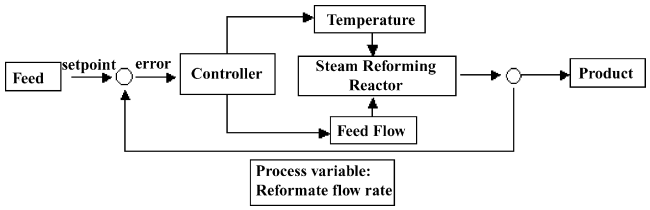

Fig. 1. Configuration of the feedback control for steam reforming reaction system.

contributed to the analysis of closed loop properties of PID controllers, focusing on system stability, robustness and performance [7,11–13].

While the use of linear models enables the PID tuning process, the underlying dynamics of specific processes can provide challenges to the use of a PID controller. In this paper, we consider PID controller for our specific MCS-based system. The unique control characteristics of MCS are evident in the different tuning parameters required by the PID controller as compared to conventional scale systems.

There have been a few reports on the incorporation of process control strategies with microreactor systems for specific control targets [6,14,15]. However, the motivations for these studies concentrated either on the framework or the theoretical approach for the implementation of actual systems rather than the realization of actual system control. We took the approach of microfabricating key components within the system, integrating each element to build a miniature plant for our specific reaction and attempting to control it experimentally. This microreactor system for steam reforming of methanol with an interconnected control algorithm is intended for use as a source of hydrogen for proton exchange membrane fuel cell (PEMFC) applications.

A schematic of the feedback control system is shown in Fig. 1 in which a control algorithm sets the reaction conditions in the MCS where a microreactor, sensors and actuators are deployed. Reformate flow rate, taken from the flow sensor in the product line, was the critical process variable to be controlled. The controller remits the output signals to the actuators depending on the set point. After determining appropriate tuning parameters, the dynamic response of the system was investigated. Detailed aspects of the MCS with regard to control characteristics were then analyzed.

2. Experimental

For fuel cell applications which have been envisioned with a portable hydrogen source, the steam reforming of methanol to produce hydrogen is attractive [16,17]. The reaction, catalyzed by $Cu/ZnO/Al_2O_3$, produces a hydrogen-rich gas at temperatures greater than 160 °C [18,19]. The product stream, after suitable clean-up, is an ideal feed for PEMFCs. A comprehensive control scheme encompassing temperature and flow in the reaction zone is, therefore, an extremely useful tool for implementing methanol-based fuel processors for effective hydrogen production.

A diluted methanol mixture with water was the feed for the SR reaction. This liquid mixture was converted to the vapor phase in a heated chamber and then directed to the mass flow controller (MFC). The vaporized feed stream was controlled by the MFC and fed to the reactor in which the flow rate and the temperature were controlled by a PID-based algorithm.

2.1. Flow and temperature control

The flow control of the microreactor system is important as the reaction conversion rate can be considerably affected by changing reactant flow rate, directly affecting residence time in the reaction zone. Furthermore, unlike a bulk chemical reactor, the microreactor under this study possesses microchannel geometry ranging a few hundred micrometers in its width. Therefore, even negligible flow changes could cause significant residence time changes and generate drift in the conversion of reactants.

The flow control of the feed stream was realized by joining a MFC in the control loop, and a microfabricated flow-sensing unit located downstream of the microreactor. The flow-sensing unit is in the order of 20 μm × 1500 μm [20], and will ultimately be a fully integrated part of the SR reactor as its fabrication sequence [24] is completely compatible with that used to generate the reactor [25]. The working principle of the flow sensor is that a centrally located resistor uses electrical power to generate heat, triggering temperature changes on the surfaces of sensing resistors on either side of the heater by the convective movement of the fluid stream being measured. These temperature changes consequently lead to resistance changes yielding a signal proportional to flow rate.

Microfabrication of the thin-film flow sensor was straightforward. An aluminum film was deposited on a Pyrex wafer surface by sputtering followed by lithography and etching. Anodic bonding of the Pyrex sensor chip to a microchannel in an underlying silicon substrate completed the integration [21]. The details of the sensor can be found in our previous paper [20]. The sensitivity, defined as a change in sense resistance for a given change in flow rate was 0.50 Ω $sccm^{-1}$ which yielded a flow rate signal adequate for the control system.

A schematic of the flow sensor with the flow control loop is shown in Fig. 2. The sense resistance signal was directly input as a process variable for the PID flow controller embedded in LabView. The testing environment was maintained at a constant temperature to avoid possible effects on the sensor.

The second element in the flow subsystem is a flow control valve. In this work, a standard MFC was used as a control valve for feed flow control. The MFC accepts an analog control voltage sent from the control PC, and modulates the MFC's control valve appropriately. Ultimately the MFC can be substituted by a microvalve using any of a number of possible approaches which have been reported [22] and in some cases commercialized [23].

A closed feedback loop for the temperature control of the reactor is shown in Fig. 2. The temperature sensor on the back of the reaction zone provides a voltage signal proportional to temperature. Based on the error ranges between the set point and the process variables, the LabView controlled PID algorithm transmits the control signal to trigger the solid-state relay, which

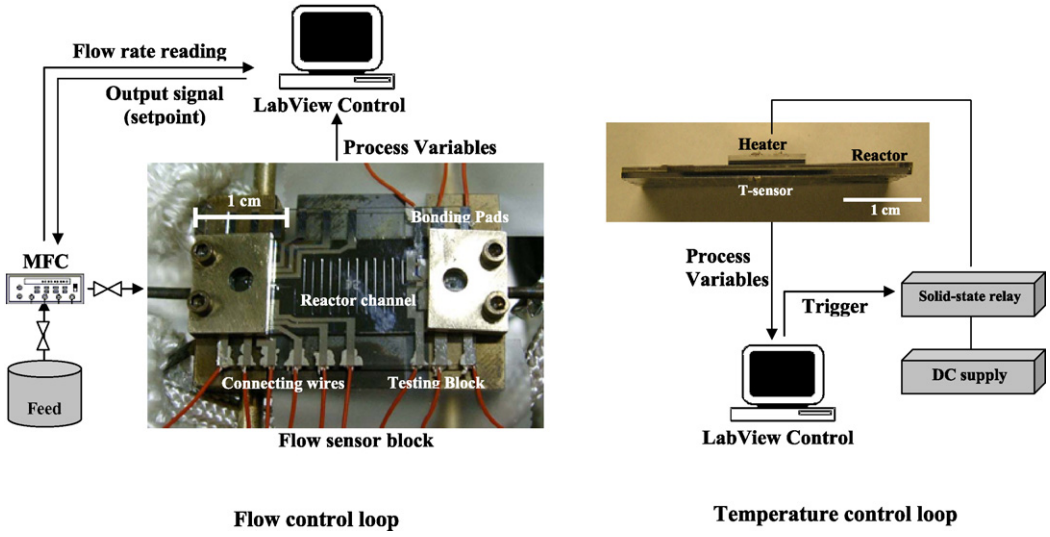

Fig. 2. Experimental schematic for flow and temperature control.

acts as an on/off switch for supplying instantaneous DC power to the heater at a varying duty cycle determined by the control algorithm.

The reaction was carried out in a silicon-based microreactor with thin-film heaters fabricated by micromachining technology [24]. A dry etching process was used to produce microgeometry in the reactor [25]. A separate heater and temperature sensor chip were attached to the reactor as shown in Fig. 3. Additional temperature sensors were fabricated in place on the back of the reactor to provide additional temperature information not used in the present experiments. Fig. 3 shows the completed reactor with individual heater and microreactor chips.

2.2. System integration

Control loops for flow and temperature in the reaction zone were then integrated to build the complete algorithm. This comprehensive control algorithm was used to control the hydrogen production rate from the MCS by manipulation of both flow and temperature. Fig. 4 shows the experimental setup for the integrated system. The flow readings of the product were used to calculate the conversion of reactants more rapidly than with the gas chromatograph (GC), which requires a cyclic measurement delay to analyze the composition of the product, and which would not be compatible to ultimate system portability. A preliminary test to calibrate the product flow rate with both conversion and hydrogen flow rate was conducted and both showed strong correlation. This flow rate was then used as the primary control target for the algorithm.

The algorithm for the integrated system is shown in Fig. 5. While the PID algorithm is usually implemented for single-input, single-output (SISO) systems, it is possible to configure a controller in single-input, multiple-output (SIMO) systems. The algorithm is composed of one input signal (H_2 flow rate) and two output signals (feed flow control, reactor temperature control). In this control loop, the control of hydrogen flow rate in the product is the target. Each controller for feed flow and reactor temperature was tuned separately to realize an acceptable

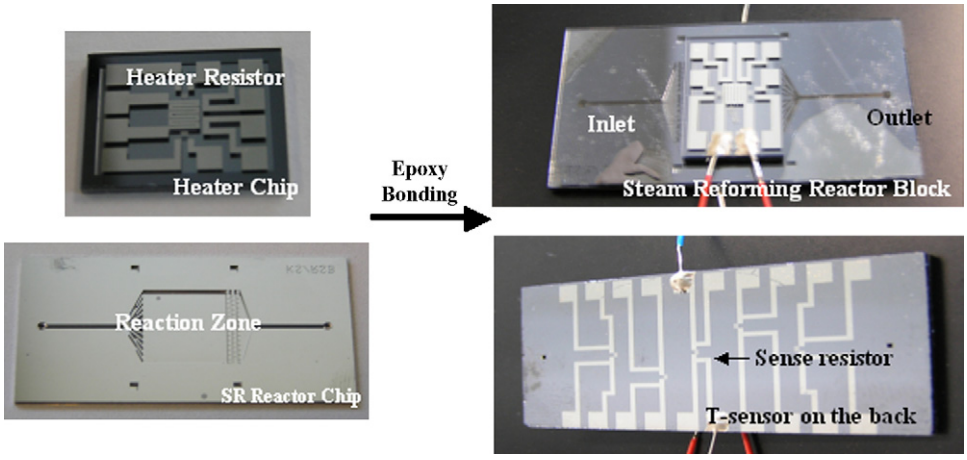

Fig. 3. Steam reforming reactor block with heater and temperature sensor.

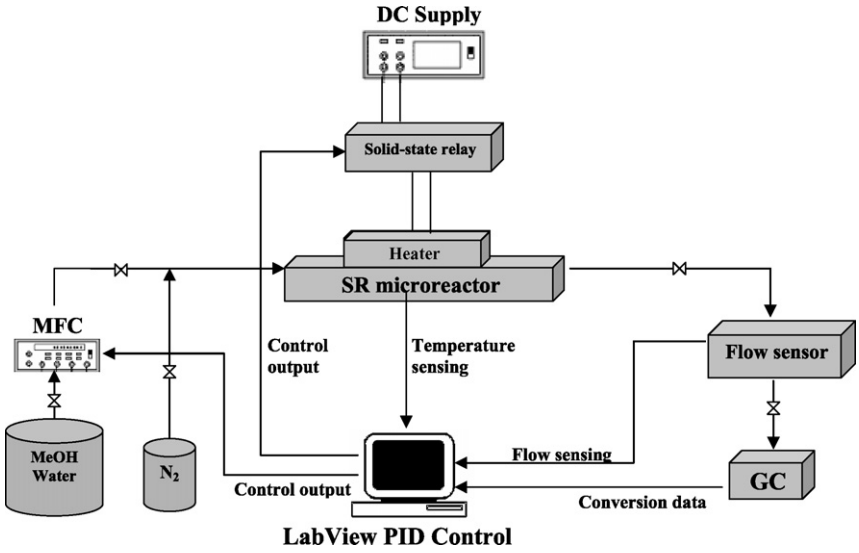

Fig. 4. Experimental schematic of integrated microreactor system. (SR microreactor system consisted of a silicon microreactor, a thin-film flow sensor, temperature sensors and thin-film heaters. Each component of the system was interfaced with LabView control software for sensing and controlling purposes.)

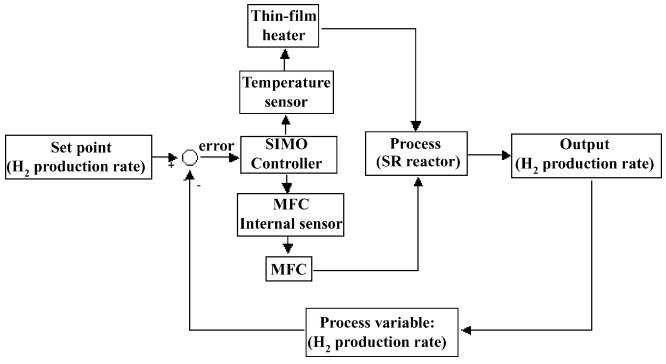

Fig. 5. Schematic representation of the implementation of the PID control algorithm for SR reaction control.

response. The flow rate of the hydrogen in the product stream is the set point in the control loop and depending on the set point defined by the operator, the algorithm remits the corresponding control signals to the controller which modulates the MFC and the solid-state relay to control the feed flow rate and the reaction temperature. In start-up, the control algorithm attempts to bring the reactor rapidly to the temperature of 260 °C, which was found to give optimal conversion and selectivity in other experiments over a broad range of flow rate [26]. The feed rate was modulated by the MFC according to hydrogen demand. A correlation between hydrogen product rate and feed flow rate was determined experimentally and was embedded in the PID algorithm as a linear function.

3. Tuning controllers

In order for PID control loops to work properly, they must be tuned for specific control targets. The need in tuning a controller is to determine the optimum values of the controller gain K_c (proportional gain), the reset time T_i and the derivative time T_d. The PID controller basically implements the following control law [27]:

$$u(t) = K_c \left(e + \frac{1}{T_i} \int_0^t e \, dt + T_d \frac{de}{dt} \right) \quad (1)$$

The controller action $u(t)$ can be calculated by the PID controller where K_c is controller gain. The controller compares the set point (SP) to the process variable (PV) to obtain an error e.

The adjustment of these tuning parameters in feedback is an important aspect of autonomous control. Standard methods for tuning loops and criteria for judging the loop tuning are well known [28–30], but have not been specifically evaluated and reported for MCS applications. In this work, the tuning rule was based on the traditional Ziegler–Nichols' (Z–N) heuristic method [11], which is a widely accepted model that generally produces reliable tuning results. Table 1 shows the detailed tuning parameters for our work.

The appropriate tuning is decided by adjusting the Z–N gains for K_c, T_i and T_d to achieve a reasonable response from the system. In this method, the T_i and T_d terms were set to zero first and the proportional gain was increased until the output of the loop oscillates. Once K_c has been set to obtain a desired fast response, the integral term was increased to stop the oscillations. The measured data (T_p, time constant; τ, dead time) for flow and temperature control were implemented in each controller (Fig. 5) to achieve a faster system response.

Table 1
Ziegler–Nichols tuning formula under PID control

Controller	K_c	T_i	T_d
PID	$1.1T_p/\tau$	2.0τ	0.5τ
Flow	16.5	4.0	1.00
Temperature	24.2	3.0	0.75
Overall	19.3	4.1	1.03

K_c, proportional gain; T_i, reset time; T_d, derivative time; T_p, time constant, τ, dead time.

4. Result and discussion

4.1. Control of individual loops

The processes we wish to control are the flow rate of the feed and the temperature in the reaction zone. In the following, we present the results for the control of the reaction to yield this target within the tuned flow and temperature control loops. In Fig. 6a, the flow rate of the feed stream was the controlled output. We see a reasonably rapid transition of the hydrogen flow to the new set point under the tuned PID controller, and stable control after reaching steady state. System rise time was about 26 s and the settling time was 50 s. The corresponding power output with the peak hydrogen production rate of 15 sccm is calculated as 1.08 W_e (overall system efficiency 60%, hydrogen utilization 75% and net efficiency 45%).

Fig. 6b shows the reaction result with a tuned temperature control loop. The feed flow was maintained at a constant value. The system rise time was about 35 s and the settling time was 75 s. As before, the corresponding power output with the peak hydrogen production rate is 1.08 W_e. The temperature dependency of the reaction is consistent with this plot. It is noticed that the system response to the changing temperature is smooth and reasonably fast (less than 100 s) and this result differentiates the microreactor from conventional bulk chemical reactors where the system temperature control requires a significantly greater time period [31].

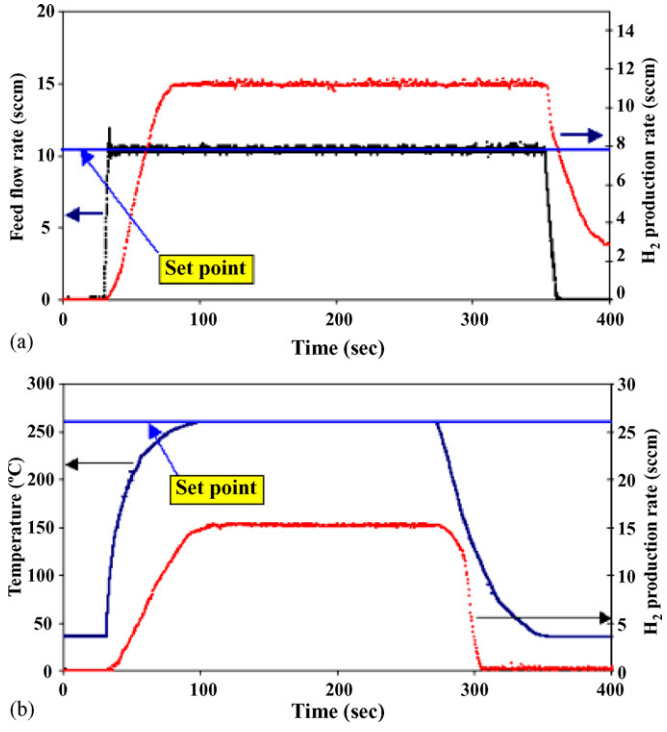

Fig. 6. SR reaction output profile with tuned PID controller. (a) Flow controlled reaction result (rise time, 26 s; settling time, 50 s) and (b) temperature controlled reaction result (rise time, 35 s; settling time, 75 s). Rise time is the amount of time the system takes to go from 10 to 90% of the final value. Settling time is the time required for the process variable to settle within a certain percentage (±5%) of the final value.

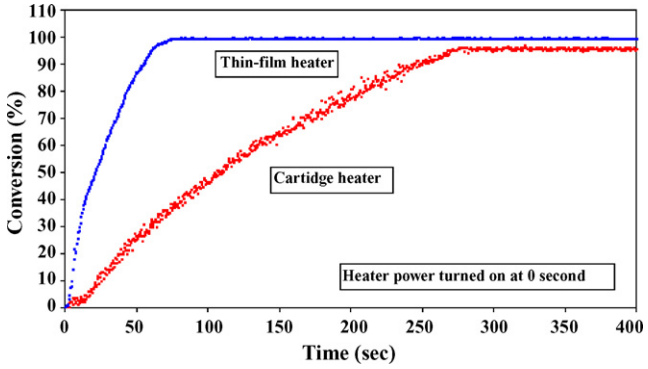

Fig. 7. SR reaction conversion comparison with thin-film and cartridge heater.

4.2. Steam reforming reaction results

The start-up behavior of miniature power sources is critical as they must compete with the nearly instantaneous turn-on behavior of typical batteries. The cold start-up behavior of the MCS for the SR reaction was tested and investigated. The control algorithm was based on the SIMO PID (in Section 3) for modulating the integrated feed and reactor temperature control (described in Fig. 5) to target a fast start-up of the system.

To compare the control characteristics of the MCS to a slightly larger scale system, a cartridge heater was introduced as the sole heating source for the microreactor block under the same reaction conditions. The conversion result in Fig. 7 demonstrates the faster system response of the MCS with integrated thin-film heater (less than 1 s). Due to the more rapid thermal stabilization in the reaction zone, the maximum conversion was reached in 70 s whereas the highest conversion with the cartridge heater was obtained after 270 s. Table 2 summarizes the different characteristics of three SR reactor systems, along with the response of a more conventional, larger scale laboratory system (Lin et al. [32]).

The first system was the MCS with an integrated heater which consisted of a silicon reactor and a thin-film heater bonded together. The second system included a commercially available cartridge heater (Omega CSS-01125) incorporated with a stainless steel block. The third system in Table 3 was a bench-scale SR reactor made of stainless steel. The faster start-up in the MCS with integrated heater is due to lower thermal mass compared to the larger systems. This fast response time of the MCS is attractive for laboratory study and small electronic systems where the system response time is crucial.

Table 2
Comparison of different systems for SR reaction

	Settling time (s)	System response (s)	Reactor dimension (cm^3)
MCS/integrated heater	70	<1	0.9
MCS/cartridge heater	270	3.0	2.5
Lin et al. [32]	1200	8.5	850

MCS/integrated heater, SR system with thin-film heater (H_2: 15.1 sccm); MCS/cartridge heater, SR system with cartridge heater (H_2: 12.6 sccm); Lin et al. [32], bench scale SR system (H_2: 91,580 sccm).

Table 3
Control characteristics of MCS for rapid load changes for the different scenarios of cellular phone operation

P_i/P_{max} (%)	P_f/P_{max} (%)	Energy (J)	T_p (s)	Dead time (s)	Settling time (s)
Start-up					
0	10	1.51	17.50	8.45	27.55
0	15	2.64	23.05	7.60	32.55
0	20	4.29	26.50	6.85	39.05
0	25	7.22	30.15	6.05	53.15
High load (calling mode)					
10	40	1.98	7.75	<0.05	9.25
15	60	3.14	5.75	<0.05	9.50
20	80	5.29	4.05	<0.05	11.50
25	100	10.73	3.50	<0.05	19.50
Low load (standby mode)					
40	10	70.26	16.25	<0.05	30.75
60	15	126.19	20.05	<0.05	35.15
80	20	230.56	28.05	<0.05	47.15
100	25	262.42	29.35	<0.05	49.05
Turn off					
10	0	–	17.50	2.00	–
15	0	–	25.50	2.00	–
20	0	–	33.45	2.05	–
25	0	–	37.55	3.05	–

P_i/P_{max}, power output ratio (initial power/maximum power); P_f/P_{max}, power output ratio (final power/maximum power); energy (J), energy needed to compensate the system lag to set point changes. For load increases, a deficit; for load decreases, an excess; T_p, time constant; dead time, time lag before the system responds; settling time, time required for the process variable to settle within a certain percentage (±5%) of the final value.

4.3. Rapid load change

The implementation of fuel cell technology requires many technical hurdles such as establishing suitable interfaces to existing systems. For example, fuel cells must possess the ability to cope with variable electronic loads which generally have nonlinear characteristics. This includes the capability to modulate the hydrogen flow for increases or decreases in electricity from the fuel cell as a constant flow of hydrogen would be wasteful in terms of system efficiency. Having a capability to meet this requirement is therefore an essential element for the fuel processor.

In Fig. 8, the MCS showed a consistent production of hydrogen when the load demand is changing. The system was controlled by the algorithm (Fig. 5) in which the hydrogen production rate is the controllable target. In this test, the set

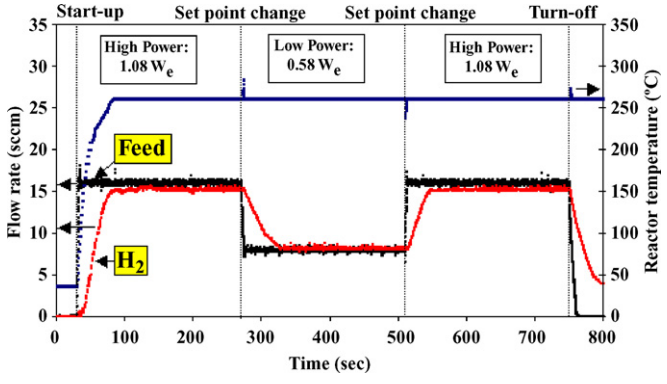

Fig. 8. Performance of SR MCS for hydrogen load changes.

production rates of hydrogen were 15.24 and 3.75 sccm which are equal to 1.10 and 0.27 W_e, respectively, of corresponding power generation. These hydrogen output rates match the power requirement of small electronic devices such as cellular phones or PDAs taking into account a net efficiency of 45%. For example, the average cellular phone's power consumption ratio is 1:4 depending on the system operation (standby mode and calling mode, respectively) [33]. Hence, the power output from the MCS is sufficient to follow the fluctuating power demand. The hydrogen production rate responds according to set point changes in the control loop and was maintained consistently with negligible disturbances. The average rise time of the system at changing set points was about 30 s as shown in Fig. 8.

For a faster system response to the changing hydrogen demand, the tuning parameters described in Table 1 were modified so that the system can more actively respond. By adjusting the integral and derivative terms (increased T_i and decreased T_d), the overshoot or undershoot were increased for each control, allowing faster transitions at the expense of short but wasteful flows and short temperature departures from the optimum. A slight increase of overshoot is frequently necessary for a fast system to respond to changes quickly [34].

As a result of this implementation, the average rise time of the system was reduced about 50% (from 30 to 15 s) as shown in Fig. 9. The shutdown response of the system was improved as well (from 130 to 45 s). The system showed good controllability for rapid load changes during the entire operation period without any noticeable instability. However, as noticed in the enlarged images in Fig. 9, the time lags when the system reacts to the load changes may not allow the fuel processor to provide sufficient output during transient conditions. To diminish these

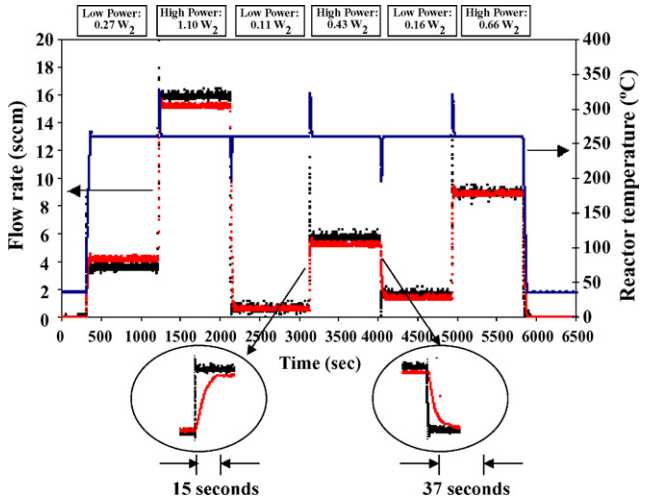

Fig. 9. Performance of SR MCS for hydrogen load changes. (Modified tuning parameters with active flow control for faster system response.)

disadvantageous effects, a ballast battery can be used to supply compensatory power during these transients. The battery is recharged during periods of steady state operation [35].

The sources of time lags in the product flow in Fig. 8 likely originate from a combination of the system holdup (time to fill system volume with reactants) and the thermal capacitance of the reactor body. To quantify these lags, the volume from the MFC to the flow sensor was measured and the time lag was estimated by dividing by flow rate. After considering the total volume between the MFC and the sensor, the calculated holdup time was about 48 s which compares well to measured the settling time (50 s) in Fig. 8. Since the volume of interconnections can be reduced significantly through full integration of microchemical components, we estimate that holdup could be reduced by at least a factor of two.

The time lag due to the thermal capacitance of the reactor in cold starting was estimated by solving a lumped thermal capacitance model [36] since the requirements for applying this model were met (the Biot number was found to be quite small; $\mathrm{Bi} \approx 10^{-7} \ll 1$). After considering the power input to the heater and the convective heat loss to the surroundings, the calculated response time from the thermal mass was about 85 s which corresponds reasonably with the measured thermal time lag in Fig. 8. This time delay is fundamental to the system as it arises from material properties and reactor dimensions. Future prototypes will likely be similar in both materials of construction and size, hence this start-up lag will need to be addressed to achieve acceptable performance.

The detailed control aspects of the MCS in relation to response to load variation are described in Table 3 for an application such as a power source for a cellular phone. The energy needed to compensate the time lag in the case when power load increases (energy column in Table 3), is less than 11 J which can easily be furnished by a commercially available miniature rechargeable battery [37]. Energies shown for demand reduction (entering the low load condition) indicate excess energy would be wasteful if not recovered to charge the battery. Thus, miniature fuel processor showed a consistent behavior with sharp fluctuations of power demand over broad ranges of power requirement.

5. Conclusion

A novel approach to understanding the behavior in an autonomous microreactor system was developed with flow and temperature control algorithms for the steam reforming of methanol. The PID-based control algorithm was implemented for the control of hydrogen production rate from the MCS. Each unit for sensing and actuating flow and temperature was interfaced with the closed loop control algorithm in LabView and communicates to attain the appropriate system control. After tuning, the controllable microreactor system showed up to 100% reaction conversion of a water–methanol mixture. The miniature steam reforming system incorporated with a comprehensive PID-based control algorithm possesses faster system start-up compared to externally heated microreactor and bench-top scale reaction systems. The system response to rapid changes of hydrogen load was improved by imposing excess overshoot to the system. System time lags during increasing load cases were quantitatively analyzed in terms of energy deficit.

Numerous research efforts have been tackled and accomplished in conjunction with the emerging miniature chemical reactor systems for utilization in fuel cell applications. As one of the essential requirements, the optimization of an overall system with autonomous control strategies is a crucial aspect. However, few attempts have been made to employ this control approach to the practical study of microreactor systems. In this regard, new control strategies must be developed for the realization of independent, autonomous microchemical system platforms. It is envisioned that eventually a single IC chip containing the control algorithm will be integrated into MCS. This study conveys the potential of MCS with integrated control for miniature, portable chemical systems.

Acknowledgements

The authors would like to thank the Micro Fabrication Center of New Jersey Institute of Technology for providing the fabrication facilities. The silicon and glass microfabrication was performed, in part, at the Cornell NanoScale Facility (a member of the National Nanofabrication Users Network) which is supported by the National Science Foundation under Grant ECS-9731293, Cornell University and industrial affiliates. Mr. Keyur Shah's generous support with fabrication and reaction characterization is also acknowledged.

References

[1] R.S. Besser, X. Ouyang, H. Surangalikar, Chem. Eng. Sci. 58 (2003) 19–26.
[2] R.S. Besser, Third Annual Tulane University Engineering Forum, New Orleans, LA, September 13, 2002.
[3] K.F. Jensen, AIChE J. 45 (10) (1999) 2051–2054.
[4] R. Srinivasan, I.-M. Hsing, P.E. Berger, M.P. Harold, J.F. Ryley, J.J. Lerou, K.F. Jensen, M.A. Schmidt, AIChE J. 43 (11) (1997) 3059–3069.
[5] C.M. Caruana, Chem. Eng. Prog. 96 (5) (2000) 9–10.

[6] O.A. Palusinski, S. Vrudhula, L. Znamirowski, D. Humbert, Chem. Eng. Prog. 97 (8) (2001) 60–66.
[7] S. Skogestad, J. Proc. Contr. 13 (2003) 291–309.
[8] P. Cominos, N. Munro, IEEE Proc. Contr. Theory Appl. 149 (2002) 17–25.
[9] M. Morari, E. Zafiriou, Robust Process Control, Prentice Hall, New Jersey, 1989.
[10] P. Mhaskar, N.H. El-Farra, P.D. Christofides, Proceedings of the 2004 American Control Conference, Boston, MA, June 30, 2006.
[11] J.G. Ziegler, N.B. Nichols, Trans. ASME 64 (1942) 759–768.
[12] J.T. Lee, W. Cho, T.F. Edgar, J. Proc. Contr. 7 (1997) 65–73.
[13] W.L. Luyben, Ind. Eng. Chem. Res. 40 (2001) 3605–3611.
[14] L.G. Bleris, J. Garcia, M.V. Kothare, M.G. Arnold, J. Proc. Contr. 16 (2006) 255–264.
[15] G. Kolb, V. Hessel, Chem. Eng. J. 98 (2004) 1–38.
[16] M.C. Williams, Advanced Fuel Cell Power Systems (http://www.fe.doe.gov/coal power/fuel cells/fc sum.html#top), viewed on 25 October 2000.
[17] B.C.H. Steele, Nature 400 (6745) (1999) 619–621.
[18] J.A. Christiansen, J. Am. Chem. Soc. 43 (1921) 1670.
[19] A.P. Meyer, J.A.S. Bett, G. Vartanian, R.A. Sederquist, US Army Technical Report DAAK70-77-C-0195, 1978.
[20] W.C. Shin, R.S. Besser, J. Micromech. Microeng. 16 (2006) 731–741.
[21] A. Cozma, B. Puers, J. Micromech. Microeng. 5 (1995) 98–102.
[22] S. Shoji, B. Van der Schoot, N. de Rooij, M. Esashi, IEEE Proceedings of Transducers '91 (1991 International Conference on Solid State Sensors and Actuators), 1991, pp. 1052–1055.
[23] A.K. Henning, J. Fitch, E. Falsken, D. Hopkins, L. Lilly, R. Faeth, M. Zdeblick, IEEE Proceedings of Transducers '97 (1997 International Conference on Solid State Sensors and Actuators), 1997, pp. 825–828.
[24] K. Shah, R.S. Besser, Proceedings of the AIChE 2006 Spring National Meeting, AIChE, Orlando, FL, 2006.
[25] R.S. Besser, W.C. Shin, J. Vac. Sci. Technol. B 21 (2) (2003) 912–915.
[26] K. Shah, R.S. Besser, J. Power Sources, submitted for publication.
[27] G. Stephanopoulos, Chemical Process Control: An Introduction to Theory and Practice, Prentice Hall, Englewood Cliffs, NJ, 1984.
[28] K.J. Astrom, T. Hagglund, Automatic Tuning of PID Controllers, Instrument Society of America, Research Triangle Park, NC, 1988.
[29] K.J. Astrom, T. Hagglund, PID Controllers: Theory, Design and Tuning, Instrument Society of America, Research Triangle Park, NC, 1995.
[30] P.J. Gawthrop, IEEE Trans. Autom. Control 31 (3) (1986) 201.
[31] Y.H. Chen, C.C. Yu, Y.C. Liu, C.H. Lee, J. Power Sources, in press (corrected proof available online on 25 April 2006).
[32] S.T. Lin, Y.H. Chen, C.C. Yu, Y.C. Liu, C.H. Lee, J. Power Sources 31 (2006) 413–426.
[33] I.V. Nicolasscu, W.F. Hoffman, Proceedings of the 2001 IEEE International Symposium on Electronics and the Environment, Denver, CO, May 7–9, 2001, pp. 134–138.
[34] G. Goodwin, S. Graebe, M. Salgado, Control System Design, Prentice Hall, Englewood Cliffs, NJ, 2001.
[35] A. Nasiri, V.S. Rimmalapudi, D.J. Chmielewski, S. Al-Hallaj, Proceedings of the 2004 IEEE Power Electronics and Motion Control Conference, The Fourth International, Beijing, China, August 14–16, 2004, pp. 491–496.
[36] F.P. Incropera, D.P. DeWitt, Heat and Mass Transfer, John Wiley & Sons, Hoboken, NJ, 2002.
[37] http://www.batteries.com/index.asp.